Extremophiles (2008) 12:351–364
DOI 10.1007/s00792-008-0139-9

ORIGINAL PAPER

Extremely thermostable esterases from the thermoacidophilic euryarchaeon *Picrophilus torridus*

Matthias Hess · Moritz Katzer · Garabed Antranikian

Received: 28 October 2007 / Accepted: 26 December 2007 / Published online: 11 March 2008

Abstract Two genes encoding esterases EstA and EstB of *Picrophilus torridus* were identified by the means of genome analysis and were subsequently cloned in *Escherichia coli*. PTO 0988, which is encoding EstA, consists of 579 bp, whereas PTO 1141, encoding EstB, is composed of 696 bp, corresponding to 192 aa and 231 aa, respectively. Sequence comparison revealed that both biocatalysts have low sequence identities (14 and 16%) compared to previously characterized enzymes. Detailed analysis suggests that EstA and EstB are the first esterases from thermoacidophiles not classified as members of the HSL family. Furthermore, the subunits with an apparent molecular mass of 22 and 27 kDa of the homotrimeric EstA and EstB, respectively, represent the smallest esterase subunits from thermophilic microorganisms reported to date. The recombinant esterases were purified by Ni^{2+} affinity chromatography, and the activity of the purified esterases was measured over a wide pH (pH 4.5–8.5) and temperature range (10–90°C). Highest activity of the esterases was measured at 70°C (EstA) and 55°C (EstB) with short *p*NP-esters as preferred substrates. In addition, esters of the non-steroidal anti-inflammatory drugs naproxen, ketoprofen, and ibuprofen are hydrolyzed by both EstA and EstB. Extreme thermostability was measured for both enzymes at temperatures as high as 90°C. The determined half-life ($t_{1/2}$) at 90°C was 21 and 10 h for EstA and EstB, respectively. Remarkable preservation of esterase activity in the presence of detergents, urea, and commonly used organic solvents complete the exceptional phenotype of EstA and EstB.

Keywords *Picrophilus torridus* · Archaea · Esterases · Hormone sensitive lipase · Thermostability · Thermoacidophilic · Nonsteroidal anti-inflammatory drugs · Organic solvents

Communicated by K. Horikoshi.

M. Hess
Genomics Division, DOE Joint Genome Institute,
Walnut Creek, CA, USA

M. Katzer · G. Antranikian (✉)
Institute of Technical Microbiology,
Hamburg University of Technology, Kasernenstr. 12,
21073 Hamburg, Germany
e-mail: antranikian@tuhh.de

Introduction

Esterases (EC 3.1.1.1) and lipases (EC 3.1.1.3) belong to a diverse group of hydrolases, catalyzing the cleavage and formation of ester bonds (Arpigny and Jaeger 1999). These lipolytic enzymes are found throughout the three phylogenetic domains of life and use a variety of substrates, which led to the assumption that they have evolved to make carbon sources accessible or to catalyze specific catabolic reaction steps (Bornscheuer 2002). The distinction between esterases and lipases is based on several characteristics of the investigated enzyme and might be continuous or even controversial in some cases (Jaeger et al. 1999; Bornscheuer 2002). In general, lipases show a preference for water-insoluble substrates, typically triglycerides composed with long chain fatty esters (≥C10), whereas esterases hydrolyze short chain acylglycerols (<C10). In this context it seems noteworthy that lipases are capable of hydrolyzing these esterase substrates as well (Jaeger et al. 1999). Lipolytic enzymes have been reported for various extremophiles including members of the order Thermoplasmatales and Sulfolobales (Suzuki et al. 2004; Golyshina et al. 2006; Mandrich et al. 2006). In recent years, the scientific and industrial significance of these extremophiles

has increased intensely due to the functional and structural stability of their proteins and due to their phylogenetic importance (Park et al. 2006). Most organisms, which proliferate at low pH values, maintain an internal pH value around neutrality. *Picrophilus*, which is able to grow at pH values comparable to 1.2 M sulphuric acid (Ciaramella et al. 2005), is one of the few microorganisms for which a low internal pH has been measured (pH 4.6) (Vossenberg et al. 1998), and it was suggested that the habitat of *Picrophilus* resembles the environment in which life originated (Di Giulio 2005). *Picrophilus torridus*, whose whole genome sequence has been published recently (Futterer et al. 2004), represents an unique model organism to study the genetic and molecular mechanisms responsible for the ability to thrive under extremely harsh conditions (optimal growth at pH 0.7 and 60°C) and a promising source of extremely stable esterases and lipases.

Despite their heterogeneous amino acid composition, α/β hydrolases share a highly conserved catalytic triad: a nucleophile (Ser, Cys, Asp), a histidine, and an acid (Asp, Glu) (Fischer et al. 2006). The region containing the active site nucleophile is usually characterized by a reasonably conserved Gly-x-[Ser/Cys/Asp]-x-Gly sequence, with 'x' indicating any amino acid. Approximately 60–108 aa upstream of this conserved pentapeptide, most esterases and lipases display a short hydrophobic region and a consensus sequence called 'the oxyanion hole' composed of a His-Gly dipeptide (Bell et al. 2002). Based on conserved sequence motifs and biological properties lipolytic enzymes can be categorized into eight families (I–VIII) and six subfamilies (I.1–I.6) within family I that contains the true lipases (Arpigny and Jaeger 1999).

Esterases and lipases are the most widely used biocatalysts in fine chemical applications, mainly because they can be applied efficiently in the production of optically pure compounds. Compared to other enzymes the industrial application of esterases is relatively mature and there is an increasing interest in high throughput tools for the discovery and characterization of these enzymes (Demirjian et al. 2001). Despite the growing interest in thermophiles and their biocatalysts, only a limited number of esterases have been characterized from thermophilic Archaea and Bacteria (Rhee et al. 2005) and all biochemically characterized esterases from thermoacidophilic microorganisms have been classified as lipolytic enzymes of family IV (synonymous to hormone sensitive lipase (HSL) family).

In this paper, we report the identification, cloning, expression, and biochemical characterization of the first esterases from the thermoacidophilic euryarchaeon *Picrophilus torridus*. Furthermore, the two purified enzymes were identified as the first esterases of family VI originated from thermoacidophiles and they displayed remarkable thermostability and chemostability.

Materials and methods

Strains and growth conditions

Picrophilus torridus DSM 9790 was obtained from the Deutsche Sammlung fuer Mikroorganismen und Zellkulturen (DSMZ) and was grown aerobically at 60°C and pH 0.7 as described in 2002 (Serour and Antranikian 2002). The medium contained (per L): 1.32 g $(NH_4)_2SO_4$, 0.28 g KH_2PO_4, 0.25 g $MgSO_4 \times 7H_2O$, 0.07 g $CaCl_2 \times 2H_2O$, 0.02 g $FeCl_3 \times 6H_2O$, 1.8 mg $MnCl_2 \times 4H_2O$, 4.5 mg $Na_2B_4O_7 \times 10H_2O$, 0.22 mg $ZnSO_4 \times 7H_2O$, and 0.05 mg $CuCl_2 \times 2H_2O$. The pH was adjusted to 0.9 with concentrated H_2SO_4. *Escherichia coli* DH5α (Invitrogen, Carlsbad, USA) was used for blue white screening of transformants containing the esterase genes from *P. torridus*. For production of the recombinant esterases, *E. coli* Rosetta™(DE3) (Novagen, Madison, USA) was used. The *E. coli* strains were cultivated aerobically in Luria Bertani (LB) (Sambrook et al. 1989). When necessary, antibiotics were supplemented to the medium to maintain the plasmids (50 mg/L carbenicillin, 50 mg/L chloramphenicol, and 50 mg/L kanamycin). Growth of all strains was analyzed by measuring the optical density (OD) at a wavelength of 600 nm.

DNA isolation and extraction

DNA from *P. torridus* was isolated by chemical lysis. Therefore, ~0.1 g of *P. torridus* cells were resuspended in 1 ml 1 M NaCl and incubated on ice for 1 h. Cells were centrifuged and the pellet was resuspended in 300 µl TE-saccharose buffer (10 mM Tris–HCl, pH 8, 1 mM EDTA, and 20% sucrose). 360 µl DNA extraction buffer (100 mM Tris–HCl, pH 8, 100 mM Na_2EDTA, 100 mM Na_2HPO_4, 1.5 mM NaCl, 1% cetyltrimethyl ammoniumbromide (CTAB), 40 µl SDS (10%) and 5 µl RNase (10 mg/mL). The mixture was incubated at 37°C for 4 h. Subsequently, 300 µl of a 5% sarcosyl solution and 10 µl proteinase K solution (10 mg/ml) were added. Samples were incubated at 37°C overnight, and DNA was extracted by phenol/chloroform standard procedure (Sambrook et al. 1989).

Cloning and expression of PTO 0988 (*estA*) and PTO 1141 (*estB*)

Open reading frames (ORFs) encoding for esterases were identified in the whole genome sequence of *P. torridus* (Futterer et al. 2004) using the ERGO software package (Integrated Genomics, Chicago, IL, USA). Genetic regions of interest were amplified in a thermocycler (Biometra,

Germany) by means of polymerase chain reaction (PCR) using *Taq* (Fermentas, Germany), *Pfu* (Fermentas, Germany), or Platinum®*Taq* DNA Polymerase High Fidelity (Invitrogen). The synthetic forward primers used for amplification of PTO 0988 (*estA*) and PTO 1141 (*estB*) were 5′-GCTAGCATGATCGATGATATGTACACAGAG G-3′, 5′-GCTAGCATGATAAGGAATTATTCTGAAAC AAGG-3′, and the reverse primers were 5′-CTCGAG TAACGATTTTGCAAAATTCACG-3′, 5′-CTCGAGTTC TATAATTTTATTTATTATTGATGAAACCTCC-3′, respectively. Primers were purchased from MWG Biotech, Germany (HPSF grade, high purity, salt free), and PCR products were analyzed at GATC Biotech (Germany) using the dideoxy chain termination method (Sanger et al. 1977). Obtained PCR products were purified using the NucleoSpin-Plasmid kit (Macherey-Nagel, Dueren, Germany) and sub-cloned into the vector pCR2.1 (Invitrogen) and pGEM-T (Promega, Madison, USA), respectively. The resulting plasmids pCR*estA* and pGEM*estB* were transformed into *E. coli* Top10 (Invitrogen), and positive clones were identified by blue/white screening followed by colony PCR. To facilitate the expression of the esterase genes the constructed plasmids pCR*estA* and pGEM*estB*, and the commercially available plasmid pET24b (Novagen) were digested with both *Nhe*I and *Xho*I. The gained DNA fragments, harboring the genes of interest, were ligated into the digested expression vector pET24b, resulting in the expression vectors pET*estA* and pET*estB*. Competent *E. coli* Rosetta (DE3) (Novagen) cells were transformed with the constructed expression vectors, and the recombinant cells were cultivated in LB media containing 50 mg/L chloramphenicol and 50 mg/L kanamycin, to confirm the successful uptake of the plasmid. Expression of *estA* and *estB* was induced with 2 and 5 mM isopropyl-thiogalactopyranoside (IPTG), respectively, after the cells reached an optical density (OD) of 0.8 at 600 nm.

DNA sequence analysis

Expression plasmids pET*estA* and pET*estB* were purified from the recombinant *E. coli* Rosetta strains, and the pure plasmids were sequenced using the BigDye Terminator v3.1 Cycle Sequencing Kit (Applied Biosystems, Foster City, CA, USA). Sequence analysis was performed using Artemis (Berriman and Rutherford 2003) and Vector NTI Advance (Invitrogen) under a private license. Chromatograms were analyzed with Chromas (Technelysium Pty Ltd, Australia). Sequence homology was investigated using NCBI-BLAST (Altschul and Lipman 1990; Altschul et al. 1997) provided by the National Center for Biotechnlology Information (NCBI), Bethesda, USA. Multiple alignments were done using ClustalW and ClustalX (Thompson et al. 1994, 1997). Nucleotide and amino acid sequences were retrieved from The Institute of Genomic Research (TIGR) (http://www.tigr.org), Genomes OnLine Database (GOLD) (GOLD 2006), and from nucleotide, genome, protein, and structure databases provided by NCBI (http://www.ncbi.nlm.nih.gov/). Additional protein sequence and protein structure information were obtained from the Braunschweig Enzyme Database (BRENDA) (Schomburg et al. 2004), the Expert Protein Analysis System (ExPASy) (Gasteiger et al. 2003), the ESTHER database (Hotelier et al. 2004), the Pfam database (Finn et al. 2006), and the Research Collaboratory for Structural Bioinformatics Protein Data Base (PDB) (Dutta and Berman 2005). PDB data for 3D modeling was calculated using automated computer algorithms (Bates et al. 2001). SignalP version 3 was used to analyze proteins for the presence of potential signal peptide sequences (Bendtsen et al. 2004), and protein structure models were visualized using the molecular viewer RasMol (Sayle and Milner-White 1995; Bernstein 2000).

Purification of the recombinant esterases

Cells were grown overnight at 30°C, harvested by centrifugation (24,000 × *g* for 30 min at 4°C), and the pellet was resuspended and washed in ice-cold 50 mM Tris–HCl buffer (pH 8). Supernatant was concentrated 20× and protein composition was examined. The cells were disrupted at 4°C by ultrasonification (Branson sonifier 450, duty cycle 40%, and output control level 4). Cell lysis was verified by light microscopy. Cell debris was removed by centrifugation (60,000 × *g* for 1 h at 4°C). The cell-free supernatant, from now on referred to as crude extract, was stored at 4°C for further analysis.

The crude extract was loaded onto an equilibrated Ni^{2+} chromatography column (Novagen). Proteins lacking a His-tag were removed by washing the column with 20 mM Tris–HCl (500 mM NaCl, 60 mM imidazole, pH 7.9), and the recombinant protein was eluted with 20 mM Tris–HCl (500 mM NaCl, pH 7.9) containing 1 M imidazole. Protein concentration of the fractions was determined spectrophotometrically after Bradford, using bovine serum albumin (BSA) as standard (Bradford 1976). The obtained elute was dialyzed against 50 mM Tris–HCl (pH 7) buffer for 40 h at 4°C.

Gel electrophoresis and Western blot analysis

SDS-PAGE was carried out with 4% polyacrylamide/12% polyacrylamide gels (stacking gel/separating gel) in a Mini Protean II electrophoresis system (Bio-Rad, Richmond,

CA, USA) (Laemmli 1970). Samples were incubated in reducing sample buffer with the following concentrations: 63 mM Tris–HCl, pH 6.8, 10% (v/v) glycerol, 0.0025% (w/v) bromphenol blue, 4% (w/v) SDS, 1.25% (w/v) dithiothreitol (DTT) at 95°C for 5 min before loading. After electrophoresis, protein bands were stained with Coomassie brilliant blue R-250. Low molecular weight marker (Amersham Biosciences) was used as standard.

Non-denaturing polyacrylamide gel electrophoresis (Non-denaturing-PAGE) was performed with gradient gels (Novex pre-cast gels, 4–20% polyacrylamide) purchased from Invitrogen. Samples were mixed with non-reducing sample buffer (final concentration 63 mM Tris–HCl, pH 8.8, 0.0025% (w/v) bromphenol blue, 10% (v/v) glycerol) before loading. High molecular weight marker (Amersham, Pharmacia) was used as a standard to estimate the subunit composition.

Detection of the His-tagged protein was carried out by Western blot analysis after the purified esterases were separated by SDS-PAGE and blotted onto a nitrocellulose membrane (Transfer buffer: 192 mM glycine, 25 mM Tris base, 20% methanol, pH 8.0). Monoclonal His-tag antibodies (IgG_1), anti-mouse IgG alkaline phosphatase conjugate, and a BCIP/NBT (5-bromo-4-chloro-3-indolyl-1-phosphate/nitro blue terazolium) staining kit (Novagen) were used and procedures were conducted according to the supplemented protocols.

Activity detection and measurement

LB plates containing 1% glyceryl tributyrate and the appropriate selective antibiotics were used to screen for positive transformants producing active recombinant EstA or EstB. 1 mM IPTG was added to the pre-warmed plates before transformants were transferred to the screening plates using sterile techniques. Plates were incubated at 37°C for up to 5 days or transferred to 50°C after 2 days at 37°C. *E. coli* Rossetta (DE3) pET24b(+) was used as negative control.

Esterase activity was measured with *para*-nitrophenyl (*p*NP)-esters as substrate (Winkler and Stuckmann 1979). The released *para*-nitrophenol was detected spectrophotometrically at 410 nm. The *p*NP-ester mixture [2 mM *p*NP-ester, 50 mM Tris–HCl (pH 7), 0.1% (w/v) gum Arabic] was pre-warmed, and the reaction was started by adding 3 U EstA or 0.14 U EstB. Hydrolysis of *p*NP-esters was carried out in 1 ml at 70°C for 30 min (EstA) or 50°C for 15 min (EstB). Reaction was terminated by addition of Na_2CO_3 to a final concentration of 10 mM and by placing the samples on ice. Samples were centrifuged for 2 min at 9,400×*g*. The amount of released *para*-nitrophenol was measured photometrically at 410 nm. For standard assay, the substrate used was 2 mM *p*NP-butyrate. One unit of enzyme was defined as the amount of enzyme resulting in the release of 1 µmol of *p*-nitrophenol per min. If not stated otherwise the values are the mean of triplicates. The extinction coefficient (ε_{410}) used was 10,350 M^{-1} cm^{-1}. Measurements were corrected for autohydrolysis of the substrate. Substrate specificity towards *p*NP-esters with *p*NP-acetate (C2), *p*NP-butyrate (C4), *p*NP-caproate (C5), *p*NP-caprylate (C8), *p*NP-decanoate (C10), *p*NP-laurate (C12), *p*NP-myristate (C14), *p*NP-palmitate (C16), and *p*NP-stearate (C18), was determined using the standard assay described before.

Hydrolysis of 4-nitrophenyl benzoate, 4-nitrophenyl 3-phenylbutanoate, 4-nitrophenyl 2-(4-isobutylphenyl) propanoate, 4-nitrophenyl 2-phenylpropanoate, 4-nitrophenyl cyclohexanoate, 4-nitrophenyl 2-(3-benzoylphenyl) propanoate, 4-nitrophenyl-2-naphthoate, 4-nitrophenyl adamantanone, 2-(4-isobutylphenyl)-N-(4-nitrophenyl) propanamide, 4-nitrophenyl 1-naphthoate, and (*S*)-4-nitrophenyl 2-(6-methoxynaphthalen-2-yl) propanoate was determined in duplicates. Reactions were carried out for 40 min with 5 mg/ml substrate in 100 mM Tris–HCl buffer (pH 7.5) at the temperature indicated in the standard assay.

Hydrolytic activity of EstA and EstB towards various triglycerides was determined at 430 nm by measuring the amount of accumulated free fatty acids in form of the corresponding copper soaps (Schmidt-Dannert et al. 1994). Enzyme samples containing the substrate were incubated under vigorous shaking for 16 h at 70°C (EstA) or 50°C (EstB), and the reaction was terminated by adding 33% (v/v) 3 M HCl. Absorption at 430 nm was measured after fatty acid extraction and addition of 1‰ (w/v) diethyldithiocarbamate. One unit of enzyme was defined as the amount of enzyme resulting in the release of 1 µmol of free fatty acids per min under reaction conditions. Measurements were corrected for autohydrolysis of the substrate.

Enzymatic assays to determinate the K_m and v_{max} values were done at different substrate concentrations, in three independent trials. Corresponding v_{max} and K_m were computed using the Michaelis–Menten equation and the BioDataFit program (Chang Bioscience, Castro Valley, USA) and the values given represent the calculated mean.

Influence of temperature and pH

Enzyme activity was determined over a temperature range from 10 to 90°C. The assays were performed at standard assay conditions. Effect of pH on esterase activity was determined over a pH range of 4–9 in 40 mM universal buffer (Britton and Robinson 1931). Measurements were corrected for autohydrolysis of the substrate.

Thermostability of the enzymes was evaluated by incubation of EstA and EstB at temperatures between 50 and 90°C for up to 24 h. Standard assays were conducted to determine the residual enzyme activity.

Effect of diverse substances on the activity of the recombinant enzymes

The influence of metal ions was investigated by adding selectively 10 mM of Al^{3+}, Ca^{2}+, Co^{2+}, Cr^{3+}, Cu^{2+}, Fe^{3+}, K^{+}, Mg^{2+}, Mn^{2+}, Na^{+}, or Ni^{2+} directly to the standard assay mixture. Enzyme activity determined in the absence of additional metal ions was defined as 100% activity.

The influence of various other substances such as inhibitors, detergents, and organic solvents was investigated using a slightly modified protocol. Prior to the standard activity assay, the enzyme (3 U/ml EstA or 0.14 U/ml EstB) was incubated for 1 h at RT in a pre-incubation mixture, containing selectively an inhibitor, detergent, or organic solvent. The reaction was performed under standard assay conditions and was initiated by addition of *p*NP-butyrate. The concentration of the additive during the standard assay was as follows: 10 mM inhibitor, 10% detergent, and 50% (v/v) or 90% (v/v) organic solvent. Concentration of urea was 1, 3, or 5 M. Enzyme activity determined for samples without additive was defined as 100% activity. Measurements were corrected for autohydrolysis of the substrate.

Sequence accession number

The *estA* and *estB* sequences are available in the GenBank database under the accession number AAT43573 and AAT43726, respectively.

Results

Identification and sequence analysis of EstA and EstB

The complete genome of *P. torridus* was analyzed for the presence of conserved regions distinctive for α/β hydrolases. This analysis revealed the presence of two ORFs, namely PTO 0988 and PTO 1141, possessing conserved regions characteristic for α/β hydrolases (Fig. 1). PTO 0988, which is encoding EstA, consists of 579 bp, whereas the EstB encoding PTO 1141 is composed of 696 bp, corresponding to 192 aa and 231 aa, respectively.

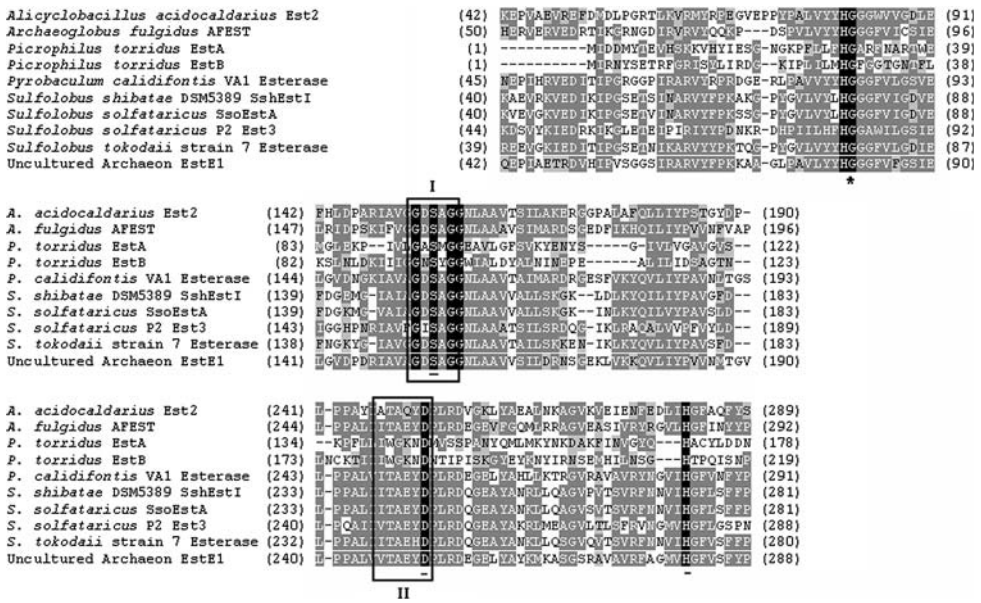

Fig. 1 Sequence comparison of *Picrophilus torridus* esterase EstA and EstB. Sequence comparison of the *P. torridus* esterase EstA and EstB with sequences from previously characterized esterases [*Alicyclobacillus acidocaldarius* Est2 (De Simone et al. 2000), *Archaeoglobus fulgidus* AFEST (Manco et al. 2000), *Pyrobaculum calidifontis* VA1 Esterase (Hotta et al. 2002), *Sulfolobus shibatae* DSM5389 SshEstI (Ejima et al. 2004), *Sulfolobus solfataricus* SsoEstA (Morana et al. 2002), *Sulfolobus solfataricus* P2 Est3 (Kim and Lee 2004), *Sulfolobus tokodaii* strain 7 Esterase (Suzuki et al. 2004), and EstE1 from an uncultured Archaeon (Rhee et al. 2005)]. Identical amino acids are *white letters on black background*. Conserved amino acids are *white letters on dark gray background*. Weakly similar amino acids are *black letters on light gray background*. Non-similar amino acids are *black letters on white background*. The oxyanion hole is indicated by an *asterisk*. Active-site residues are *underlined*. The Gly-x-Ser-x-Gly region containing the active serine residue is located in *Box I*. The conserved Ile-Trp-Gly-Lys-Asn-Asp hexapeptide of EstA and EstB is located in *Box II*

Multiple sequence alignment of the EstA and EstB sequences with amino acid sequences from previously characterized esterases suggests the presence of the oxyanion hole (His-Gly) at position 29/30 (EstA) and 28/29 (EstB). A Gly-x-Ser-x-Gly region containing the active serine residue was identified in EstA and EstB from Gly92 to Gly96 and Gly93 to Gly97, respectively. The Asp and His residues of the putative catalytic triad were predicted to be located at position 144 and 171 for EstA and at position 185 and 212 for EstB. Furthermore, an additional conserved Ile-Trp-Gly-Lys-Asn-Asp hexapeptide containing the catalytic Asp residue was identified in the EstA and EstB sequences at position 139 to 144 (EstA) and 180 to 185 (EstB) (Fig. 1). Both EstA and EstB possess an extremely low sequence identity to other previously described esterases, and sequence identity with each other amounts only to 16%. Further analyses indicate that EstA shares 11, 14, 14, 14, 14, 11, 12, and 13% sequence identity with *Alicyclobacillus acidocaldarius* Est2 (De Simone et al. 2000), *Archaeoglobus fulgidus* AFEST (Manco et al. 2000), *Pyrobaculum calidifontis* VA1 esterase (De Simone et al. 2000; Hotta et al. 2002), *Sulfolobus shibatae* SshEst1 (Ejima et al. 2004), *S. solfataricus* SsoEstA (Morana et al. 2002), *S. solfataricus* Est3 (Kim and Lee 2004), *S. tokodaii* esterase (Suzuki et al. 2004), and with the characterized esterase EstE1 isolated from a metagenomic library (Rhee et al. 2005), respectively. EstB shares 16, 12, 12, 14, 13, 10, 14, and 12% sequence identity correspondingly. These results were supported by the results of an autonomous database search against published 3D protein structures. An α/β hydrolase fold for EstA was predicted between residue 52 and 156 and between residue 48 and 228 for EstB. Additional computational 3D structure modeling of EstA and EstB indicate the presence of the canonical central sheet consisting of eight parallel β-strands connected by α-helices (data not shown). Neural networks (NN) and hidden Markov models (HMM) implemented with SignalP predicted no potential signal peptide sequence for either EstA or EstB. In addition, analysis of the EstA and EstB sequences and comparison to previously characterized esterases suggest that both esterases from *P. torridus* are members of family VI. Interestingly, all other previously described esterases from thermoacidophiles are members of the HSL family (family IV) characterized by a conserved His-Gly-Gly-Gly/Ala oxyanion hole sequence and a conserved Gly-x-Ser-Ala-Gly-Gly hexapeptide containing the active serine (Fig. 1) (Arpigny and Jaeger 1999; Kim and Lee 2004; Mandrich et al. 2006). A conserved Ile-Trp-Gly-Lys-Asn-Asp hexapeptide containing the catalytic Asp residue was identified in the EstA and EstB sequences at position 139 to 144 and 180 to 185, respectively.

DNA isolation, cloning of *estA* and *estB*, and subsequent transformation of *E. coli* cells

Genomic DNA was isolated successfully from *P. torridus* by chemical lysis, and the protein-free product was used as a template for PCR-based amplification of ORF PTO 0988 and ORF PTO 1141, and the yielded PCR products were in the desired size range size of 588 bp (ORF PTO 0988) and 705 bp (ORF PTO 1141). The PCR products were purified and cloned successfully in the plasmids pCR2.1 TOPO TA and pGEM-T AccepTor, respectively, and the constructed plasmids (pCR*estA* and pGEM*estB*) were transformed into electrocompetent *E. coli* cells. Subsequently, transformants carrying the DNA fragment of interest were identified by blue/white screening. Additional restriction sites within the PCR products allowed a selective double digestion by the restriction endonucleases *Xho*I and *Nhe*I. Successful purification from the amp resistant transformants and double digestion of pCR*estA* and pGEM*estB* were verified by size fractionating on an agarose gel. Additionally, preparative size fractionating confirmed the successful double digestion of the expression vector pET24b(+) with *Xho*I and *Nhe*I. The fragments *estA* and *estB* derived from pCR*estA* and pGEM*estB* were ligated in the double digested pET24b(+), and the constructed plasmids (pET*estA* and pET*estB*) were transformed into electrocompetent *E. coli* Rosetta (DE3) cells. Transformants carrying the DNA fragment of interest were identified by growth on selective LB plates and about 2,000 single colonies were transferred to screening plates containing tributyrate as substrate. Although tributyrate hydrolysis at 37°C was observed for 93% of the clones, halo formation around the CFUs was extremely weak and took as long as 5 days. No halos were observed for clones incubated at 37°C for 2 days and subsequently transferred to 50°C. Individual clones selected for further investigation were subjected to plasmid purification. Successful purification was confirmed by agarose gel electrophoresis. Subsequent determination of the insert specific sequence by the dideoxy chain termination method (Sanger et al. 1977) verified that both *estA* and *estB* were cloned successfully into the expression vector pET24b(+).

Expression of recombinant *estA* and *estB*

Production of soluble esterases was achieved by gene expression induced by 2 mM (EstA) or 5 mM (EstB) IPTG. Esterase activity was detected after harvesting and preparation of the crude extract for *E. coli* Rosetta (DE3) pET*estA* and *E. coli* Rosetta (DE3) pET*estB*. Ester hydrolysis was detected with the spectrophotometrical standard assay, and measurements of *p*NP-ester hydrolysis were corrected with

E. coli Rosetta (DE3) pET24b(+) crude extract as negative control. Specific esterase activity of 3.65 U/mg was determined for *E. coli* Rosetta (DE3) pET*estA* crude extract and of 5.17 U/mg for *E. coli* Rosetta (DE3) pET*estB* crude extract. SDS-PAGE was used to analyze the protein pattern of supernatant and crude extract prepared from Rosetta (DE3) pET*estA*, Rosetta (DE3) pET*estB*, and Rosetta (DE3) pET24b(+). An additional band was found in the samples of Rosetta (DE3) pET*estA* and Rosetta (DE3) pET*estB* crude extracts, and a molecular mass of 22 kDa (EstA) and 27 kDa (EstB) was calculated from the migration length R_f of the proteins (Data not shown).

Purification of EstA and EstB and kinetic studies

The recombinant esterases were purified in an extremely efficient one-step purification procedure using Ni^{2+} affinity chromatography. Results of the purification procedure of EstA and EstB are summarized in Table 1. 92% of the initial total activity and a specific activity of 32.6 U/mg were measured for purified EstA, after the samples had been pooled and dialyzed, commensurating to an 8.9-fold purification factor. In contrast, the purification factor of EstB was 510-fold and therefore significantly (57 times) higher. After the purification of EstB, 90% of the initial total activity (126 U) was recovered and the purified esterase had a remarkably high specific activity (2,639 U/mg).

SDS-PAGE and native-PAGE of purified EstA and EstB were performed to confirm the homogeneous purification and to determine the molecular mass of the recombinant proteins under denaturing and non-denaturing conditions. Results obtained from both SDS-PAGE (Fig. 2) and native-PAGE (Fig. 3) verified that Ni^{2+} chromatography was used efficiently to purify both EstA and EstB to homogeneity. Furthermore, the results suggest that both active esterases are homotrimers composed of subunits with a molecular mass of 22 kDa (EstA) and 27 kDa (EstB) each.

Table 1 Purification of EstA and EstB

Purification step	Total protein (mg)	Total activity (U)	Specific activity (U/mg)	Yield (%)	Purification factor (fold)
a. EstA					
Crude extract	51	185	3.65	100	1
Ni^{2+} column	5.3	171	32.58	92	8.9
b. EstB					
Crude extract	24.4	126.25	5.17	100	1
Ni^{2+} column	0.043	113.5	2,639	90	510.5

Western blot analysis revealed the presence of the six C-terminal His residues (data not shown), which is not surprising, as Ni^{2+} affinity chromatography was used successfully for purification of the recombinant proteins.

The v_{max} and K_m of EstA and EstB were determined with *p*NP-butyrate as substrate, using the spectrophotometrical standard assay. v_{max} and K_m of EstA are 2,934.78 U/mg and 2.9 mM. The corresponding v_{max} and K_m values for EstB are 2.2×10^6 U/mg and 2.35 mM.

Esterase activity towards pNP-esters and triglycerols

Substrate specificity of the recombinant esterases towards *p*NP-esters was determined as described in the Materials and methods section, and the results are summarized in Table 2. Both esterases are active against short *p*NP-esters, with *p*NP-acetate as the most favored substrate. Specific activity of EstA and EstB towards *p*NP-acetate was 41 and 3,306 U/mg, respectively. Specific activity of EstA and EstB towards the less autohydrolyzing *p*NP-butyrate was found to be 20% less. The specific activity was further reduced with *p*NP-caproate as substrate. Hydrolytic activity towards *p*NP-caprylate was measured solely for EstA, but not for EstB. *p*NP-esters with longer acyl chains, such as *p*NP-caprylate, *p*NP-laurate, *p*NP-myristate, *p*NP-palmitate, and *p*NP-stearate were not hydrolyzed by either EstA or EstB. As further results indicate, both recombinant esterases are possessing

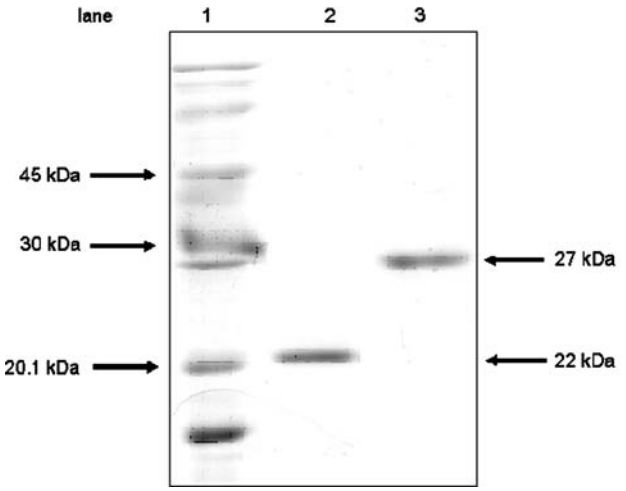

Fig. 2 SDS PAGE of purified EstA and EstB. Molecular mass of purified EstA and EstB under denaturing conditions was determined by SDS-PAGE. Sample containing 1 μg of EstA and EstB were loaded to lane 2 and lane 3, respectively. After electrophoresis and protein staining, a single band of 22 and 27 kDa was visible in lane 2 and lane 3, respectively. Lane 1 contains the LMW marker (Amersham, Germany) with the standard proteins as follows: phosphorylase b (97 kDa), bovine serum albumin (66 kDa), ovalbumin (45 kDa), carbonic anhydrase (30 kDa), trypsin inhibitor (20.1 kDa), and α-lactalbumin (14.4 kDa)

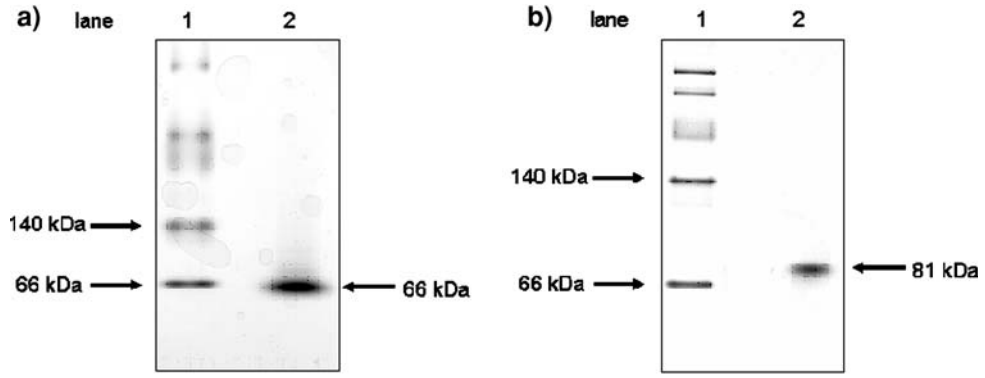

Fig. 3 Non-denaturing PAGE of purified EstA and EstB. 3 μg of EstA was loaded to lane 2a (**a**) and 1.3 μg of EstB was loaded to lane 2b (**b**), respectively. After electrophoresis and protein staining, a single band of 66 and 81 kDa was visible in lane 2a and lane 2b, respectively. Lane 1 of both **a** and **b** contains the HMW native marker (Amersham, Germany) with the standard proteins as follows: thyroglobulin (669 kDa), ferritin (440 kDa), catalase (232 kDa), lactate dehydrogenase (140 kDa), and albumin (66 kDa)

Table 2 Substrate specificity of EstA and EstB

Substrate	Specific activity of EstA (U/mg)	Specific activity of EstB (U/mg)
*p*NP-acetate (C2)[a]	41	3,306
*p*NP-butyrate (C4)[a]	33	2,639
*p*NP-caproate (C5)[a]	17	696
*p*NP-caprylate (C8)[a]	11	0
*p*NP-decanoate (C10)[a]	0	0
*p*NP-laurate (C12)[a]	0	0
*p*NP-myristate (C14)[a]	0	0
*p*NP-palmitate (C16)[a]	0	0
*p*NP-stearate (C18)[a]	0	0
*p*NP-adamantanone[b]	0	0
*p*NP-benzoate[b]	0	0
*p*NP-cyclohexanoate[b]	5.2	27.7
*p*NP-1-naphthoate[b]	0.27	0
*p*NP-2-naphthoate[b]	0	0
*p*NP-2-(3-benzoylphenyl) propanoate[b]	3.1	3.12
*p*NP-2-(4-isobutylphenyl) propanoate	6.92	0.28
*p*NP-2-phenylpropanoate[b]	5.72	33.61
*p*NP-3-phenylbutanoate[b]	1.86	6.95
(*S*)-*p*NP-2-(6-methoxynaphthalen-2-yl) propanoate[b]	1.2	1.28
2-(4-isobutylphenyl)-N-*p*NP-propanamide[b]	0	0

[a] The *p*NP-ester mixture [2 mM *p*NP-ester, 50 mM Tris–HCl (pH 7), 0.1% (w/v) gum Arabic] was pre-warmed prior to addition of 3 U/ml EstA or 0.14 U/ml EstB. Hydrolysis of *p*NP-esters was carried out at 70°C for 30 min (EstA) or at 50°C for 15 min (EstB)

[b] The *p*NP-ester mixture [5 mg/ml *p*NP-ester, 100 mM Tris–HCl (pH 7.5), 0.1% (w/v) gum Arabic] was pre-warmed prior to addition of 3 U/ml EstA or 0.14 U/ml EstB. Hydrolysis of *p*NP-esters was carried out for 40 min at 70°C (EstA) or 50°C (EstB)

hydrolytic activity towards 4-nitrophenyl 2-(4-isobutylphenyl) propanoate, 4-nitrophenyl 2-(3-benzyphenyl) propanoate, and (*S*)-4-nitrophenyl 2-(6-methoxynaphthalen-2-yl) propanoate. 4-nitrophenyl 2-(4-isobutylphenyl) propanoate, 4-nitrophenyl 2-(3-benzoylphenyl) propanoate, and (*S*)-4-nitrophenyl 2-(6-methoxynaphthalen-2-yl) propanoate are *p*NP-esters of the drugs distributed under the commercial name ibuprofen, ketoprofen, and naproxen, respectively. EstA and EstB were able to hydrolyze 4-nitrophenyl 2-phenylpropanoate, 4-nitrophenyl cyclohexanoate, and 4-nitrophenyl cyclohexanoate as substrate. Hydrolysis of 4-nitrophenyl-1-naphthoate was only observed for EstA.

Hydrolytic activity of the purified recombinant esterases towards triglycerols (i.e. triacetate, tributyrate, tricaprylin, trimyristin, tripalmitin, and tristearin) was examined, and no activity towards these substrates was measured for either EstA or EstB (data not shown).

Influence of temperature and pH

Activity of the recombinant esterases was investigated over a temperature range from 10 to 90°C using the spectrophotometrical standard assay with 2 mM *p*NP-butyrate as substrate. The derived results (Fig. 4) indicate that both enzymes are active over a broad temperature range and highest hydrolytic activity was measured at 70 and 55°C for EstA and EstB, respectively. In the temperature range corresponding to the temperature found in the habitat of *P. torridus* (55°C) both esterases exhibit >50% relative activity. No activity was found for EstA at 30°C and below, whereas 20% relative activity was measured for EstB at 10°C. Both enzymes were found to be extremely thermostable for 24 h at temperatures as high as 90°C. More precisely, at 90°C EstA and EstB displayed a half-life of 21 and 10 h, respectively (Fig. 5).

Hydrolytic activity of EstA and EstB was analyzed between pH values of 4 and 9 using the standard assay and 40 mM universal buffer containing phosphoric, acetic, and boric acid. Maximal activity of EstA and EstB was measured at pH 6.5 and pH 7, respectively. Activity was detected for both enzymes over the complete range of pH values examined (Fig. 6). EstA showed 2.6% relative activity at pH 4 and 1.5% relative activity at pH 9. EstB showed 0.2% relative activity at pH 4 and 0.5% relative activity at pH 9.

Effect of metal ions, detergents, and other denaturing agents

The effect of various metal ions was investigated by performing the standard esterase assay in the presence of either 10 mM Al^{3+}, Ca^{2+}, Co^{2+}, Cr^{3+}, Cu^{2+}, Fe^{3+}, K^{+}, Mg^{2+}, Mn^{2+}, Na^{+}, or Ni^{2+} (Table 3). It was found that both enzymes were not affected significantly by either Ca^{2+} or Na^{+}. Al^{3+} reduced solely the relative activity of EstB to 88%, whereas the activity of EstA was not affected. The presence of Co^{2+}, Cr^{3+}, Cu^{2+}, Fe^{3+}, and Ni^{2+} ions had an inhibitory effect on both EstA and EstB, and it is noteworthy that activity of EstA was reduced to a greater extent by Co^{2+}, Cr^{3+}, Cu^{2+}, and Fe^{3+}, when compared to the activity of EstB. Supplementation of 10 mM Ni^{2+} caused a reduction in activity of 30% for EstA and EstB. While esterase activity of EstA and EstB was increased by the addition of Mg^{2+} and Mn^{2+}, K^{+} had a stimulating effect on EstB but reduced the activity of EstA.

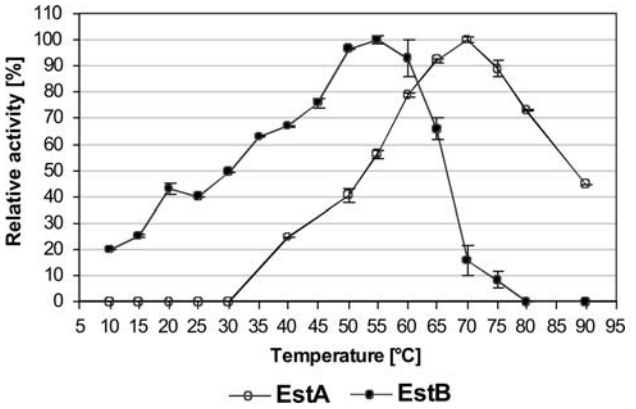

Fig. 4 Temperature profile of EstA and EstB. Enzyme activity of EstA (*o*) and EstB (•) was determined over a temperature range from 10 to 90°C. The *p*NP-butyrate mixture [2 mM *p*NP-butyrate, 50 mM Tris–HCl (pH 7), 0.1% (w/v) gum Arabic] was pre-warmed prior to addition of the enzyme. Hydrolysis of *p*NP-butyrate was carried out for 30 min (EstA) or 15 min (EstB). Reaction was terminated by addition of Na_2CO_3 to a final concentration of 10 mM and by placing the samples on ice. Measurements were done in triplicates

The effect of nonionic (Tween20, Tween80, and Triton-X100), zwitterionic (CHAPS), and ionic (SDS) detergents on esterase activity was investigated by pre-incubation of EstA and EstB in the presence of a sole detergent, prior to the standard assay. Zwitterionic 3-[(3-cholamidopropyl) dimethylammonio]-1-propanesulfonate (CHAPS) reduced the activity of EstA and had a slight positive effect on EstB. It was non-pivotal, if the detergent was ionic or non-ionic. All other detergents reduced the esterase activity of both recombinant enzymes to at least 50%, when compared to the activity of the negative control, which did not contain any detergent (Table 3).

Furthermore, the effect of various inhibitors and denaturing agents was investigated (Table 3). Activity of EstA and EstB was not affected significantly by pre-incubation with urea in concentrations as high as 5 M. 10 mM of guanidine hydrochloride reduced the activity of EstA and EstB to 53 and 70%, respectively. The chelating agent ethylenedinitrilotetraacetic acid (EDTA) had little inhibitory effect on EstA and EstB. After pre-incubation in the presence of 10 mM EDTA, a relative activity of 79% for

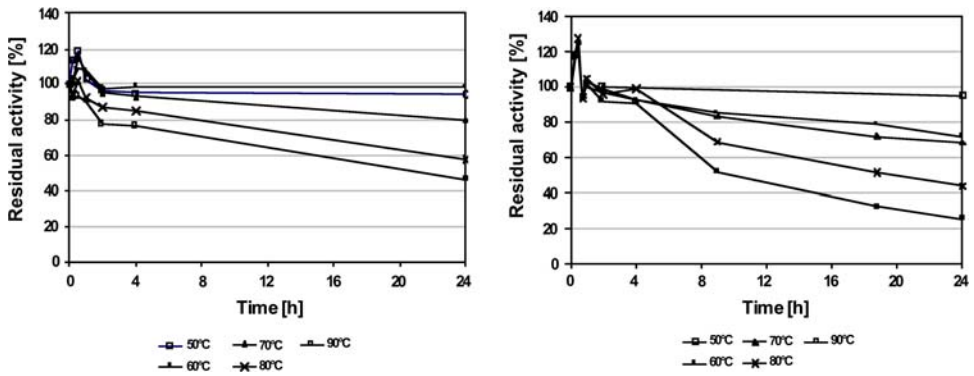

Fig. 5 Temperature stability of EstA and EstB. Thermostability of EstA (**a**) and EstB (**b**) was determined by pre-incubation of the esterases at pH 7 and different temperatures between 50 and 90°C for up to 24 h. Standard assays with 2 mM *p*NP-butyrate (EstA: 70°C, 30 min, 50 mM Tris–HCl, pH 7; EstB: 50°C, 15 min, 50 mM Tris–HCl, pH 7) were conducted periodically to determine the residual enzyme activity. Reaction was terminated by addition of Na_2CO_3 to a final concentration of 10 mM and by placing the samples on ice. The amount of released *para*-nitrophenol was measured photometrically at 410 nm. Measurements were done in triplicates and corrected for autohydrolysis of the substrate

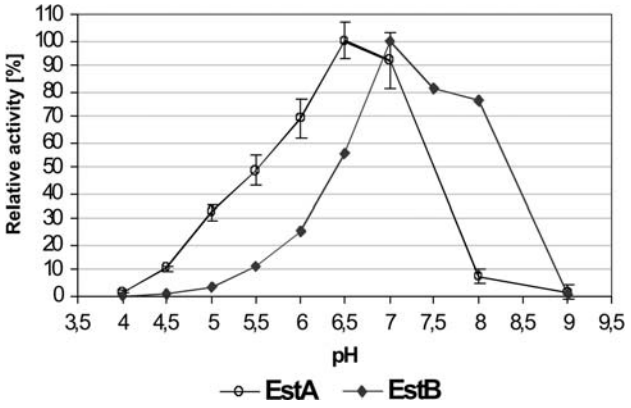

Fig. 6 pH profile of EstA and EstB. Enzyme activity of EstA (*o*) and EstB (♦) was determined over a pH from 4–9 using 40 mM universal buffer (Britton and Robinson 1931). The *p*NP-butyrate mixture [2 mM *p*NP-butyrate, 0.1% (w/v) gum Arabic] was pre-warmed prior to addition of the enzyme. Hydrolysis of *p*NP-butyrate was carried out at 70°C for 30 min (EstA) or 50°C for 15 min (EstB). Reaction was terminated by addition of Na_2CO_3 to a final concentration of 10 mM and by placing the samples on ice. Measurements were done in triplicates

EstA and 93% for EstB was measured. Reagents interacting with cysteine (2-iodoacetate and PCMB) or serine residues (Pefabloc and PMSF) reduced the ability of both enzymes to hydrolyze *p*NP-esters significantly. The disulfide reducing agents *β*-mercaptoethanol and *threo*-1,4-dimercapto-2,3-butanediol (DTT) were exceptionally efficient in reducing the activity of EstA and EstB. Only 7 and 13% of relative activity was measured for EstA and EstB, respectively, in the presence of 10 mM DTT. 10 mM *β*-mercaptoethanol inhibited EstA completely, whereas EstB was found to retain 7% of its activity.

Effect of organic solvents

Solvents are used in many industrial enzymatic bioconversions and therefore the effect of polar and non-polar solvents on the activity of the recombinant esterases is of special interest. In general, both esterases are not affected significantly by incubation with 50% (v/v) of polar solvents (Table 4). Considerable effect was measured solely in the presence of 50% (v/v) isopropanol and 50% (v/v) pyridine for EstA and in the presence of 50% (v/v) tertiary butanol for EstB. More precisely, EstA retained 63% of its activity in the presence of isopropanol and 6% of its activity in the presence of pyridine. Furthermore, EstB retained 53% of its activity in the presence of 50% (v/v) tertiary butanol. In contrary, addition of 90% (v/v) acetone, DMSO, ethanol, and pyridine resulted in a complete loss of activity of EstA. In general, EstB was found to be less susceptible to the specific additives, when compared to EstA. Tertiary butanol [90% (v/v)] had the most impact on EstB and a reduction for 63% was determined. Interestingly, the addition of 90% (v/v) dimethylformamide and 90% (v/v) tertiary butanol enhanced the activity of EstA for 65% and 13%, respectively. Non-polar solvents had a much more distinct effect on the esterases (Table 4). Relative activity of EstB was reduced below 25% in the presence of the non-polar solvents used during this study, but did not decline below 3%, which was measured in the presence of n-decyl

Table 3 Effect of various reagents

Compound	Concentration	Relative activity of EstA (%)	Relative activity of EstB (%)
None	–	100	100
Al^{3+}	10 mM	100	88
Ca^{2+}	10 mM	104	104
Co^{2+}	10 mM	75	82
Cr^{3+}	10 mM	60	85
Cu^{2+}	10 mM	42	71
Fe^{3+}	10 mM	20	64
K^{+}	10 mM	95	108
Mg^{2+}	10 mM	114	110
Mn^{2+}	10 mM	104	110
Na^{+}	10 mM	101	99
Ni^{2+}	10 mM	71	69
CHAPS	10% (w/v)	73	104
SDS	10% (w/v)	29	29
Triton-X100	10% (v/v)	31	44
Tween20	10% (v/v)	42	50
Tween80	10% (v/v)	38	40
2-Iodoacetate	10 mM	27	30
DTT	10 mM	7	13
EDTA	10 mM	79	93
Guanidine-HCl	10 mM	53	70
PCMB	10 mM	35	24
Pefabloc	10 mM	55	66
PMSF	10 mM	48	42
ß-Mercaptoethanol	10 mM	0	7
Urea	1 M	103	99
	3 M	95	98
	5 M	91	94

Prior to the standard activity assay, the enzymes (3 U/ml EstA or 0.14 U/ml EstB) were incubated for 1 h at RT in a pre-incubation mixture, containing selectively a metal salt, a detergent, an inhibitor, or a denaturing agent. The reaction was initiated by addition of 2 mM *p*NP-butyrate. Hydrolysis of *p*NP-butyrate was carried out in 50 mM Tris–HCl (pH 7) containing 0.1% (w/v) gum Arabic at 70°C for 30 min (EstA) or at 50°C for 15 min (EstB). Reaction was terminated by addition of Na_2CO_3 to a final concentration of 10 mM and by placing the samples on ice. Enzyme activity determined in the absence of detergents, inhibitors, and denaturing agents was defined as 100% activity

Table 4 Effect of organic solvents

Compound	Concentration (%)	Relative activity of EstA (%)	Relative activity of EstB (%)
None	–	100	100
Acetone	50 (v/v)	82	98
	90 (v/v)	0	84
Dimethylformamide	50 (v/v)	72	82
	90 (v/v)	165	64
DMSO	50 (v/v)	77	95
	90 (v/v)	0	75
Ethanol	50 (v/v)	77	99
	90 (v/v)	0	91
Isopropanol	50 (v/v)	63	95
	90 (v/v)	53	78
Methanol	50 (v/v)	78	98
	90 (v/v)	27	89
Pyridine	50 (v/v)	6	71
	90 (v/v)	0	50
Tert. butanol	50 (v/v)	71	53
	90 (v/v)	113	37
Amylalcohol	90 (v/v)	0	7
Benzol	90 (v/v)	43	7
Chloroform	90 (v/v)	33	16
Formaldehyde	90 (v/v)	0	10
Heptane	90 (v/v)	0	21
Hexadecane	90 (v/v)	61	17
Isooctane	90 (v/v)	0	4
n-Decyl alcohol	90 (v/v)	0	3
n-Hexane	90 (v/v)	43	23
Toluol	90 (v/v)	199	15

Prior to the standard activity assay, the enzymes (3 U/ml EstA or 0.14 U/ml EstB) were incubated for 1 h at RT in a pre-incubation mixture, containing one solvent. The reaction was initiated by addition of 2 mM *p*NP-butyrate. Hydrolysis of *p*NP-butyrate was carried out in 50 mM Tris–HCl (pH 7) containing 0.1% (w/v) gum Arabic at 70°C for 30 min (EstA) or at 50°C for 15 min (EstB). Reaction was terminated by addition of Na_2CO_3 to a final concentration of 10 mM and by placing the samples on ice. Enzyme activity determined in the absence of solvents was defined as 100% activity

alcohol. EstA, on the other hand, was inactivated completely by amylalcohol, formaldehyde, heptane, isooctane, and n-decyl alcohol. Similar to 90% (v/v) dimethylformamide, 90% (v/v) toluol enhanced the activity of EstA (199% relative activity).

Discussion

In spite of the low sequence identity, computational 3D structure modeling of the putative esterases suggests the presence of the canonical central β-sheet consisting of eight parallel β-strands connected by α-helices, which are located on the sides of the β-sheet. This structure is also known as the α/β hydrolase fold, and its precise structure varies among the different enzymes (Jaeger et al. 1999). A conserved Ile-Trp-Gly-Lys-Asn-Asp hexapeptide containing the catalytic Asp residue was identified in the EstA and EstB sequences at position 139 to 144 and 180 to 185, respectively. To date, there has been no report on the contribution of this conserved hexapeptide. Considering that the His and Asp residues of the catalytic triad stabilize the serine-bound substrate during ester hydrolysis (Bornscheuer 2002), it seems likely that the conserved hexapeptide of *P. torridus* EstA and EstB might contribute to the stabilization of the formed tetrahedral intermediate and therefore represent a codetermining factor for the specific properties of these esterases. The catalytic triad conserved in esterases contains an active serine residue and therefore serine inhibitors such as Pefabloc and phenylmethylsulfonyl fluoride (PMSF) inhibit the activity of these serine hydrolases. This was substantiated by the inhibition of EstA and EstB in the presence of 10 mM Pefabloc and PMSF. Inhibition in the presence of PMSF was also observed for the thermostable esterase Est1 and Est2 from *A. acidocaldarius* (Manco et al. 1998, 1994), the thermostable esterase from *S. acidocaldarius* (Sobek and Gorisch 1988), and the thermostable SsoP1 (Park et al. 2006). In contrast, the lipase from *Acinetobacter calcoaceticus* was not inhibited by PMSF, possibly caused by an active serine buried deeply in the molecule (Dharmsthiti et al. 1998). There is increasing evidence that disulphide bridges are essential for the functionality of some esterases. Accordingly, addition of DTT inhibited the recombinant esterase Est1 from *A. acidocaldarius* (Manco et al. 1994). The cysteine modifying reagents 2-iodoacetate and PCMB inhibited the esterase activity of EstA and EstB, suggesting that Cys174 of EstA and Cys175 of EstB might be crucial for maximal activity of these esterases.

The broad substrate specificity of these robust enzymes is remarkable and they can be of use to produce a diverse range of high-value products. Nonsteroidal anti-inflammatory drugs (NAID) are widely used for treatment of human diseases and stereoselective hydrolysis of their esters proved as a good procedure for their production (Margolin 1993). Esterification with 1-propanol of the racemic mixture has been used successfully to optimize enantioselective resolution of racemic ibuprofen (Carvalho et al. 2006). Esters of the NAID naproxen [2-(6-methoxynaphthalen-2-yl) propanoate], ketoprofen [4-nitrophenyl 2-(3-benzoylphenyl) propanoate], and ibuprofen [(4-isobutylphenyl) propanoate] were hydrolyzed by both EstA and EstB. Considering the determined specific activities, the extreme temperature stability, and the resistance towards numerous organic solvents, EstA represents a promising biocatalyst

for production and/or optimization of ibuprofen and naproxen. EstB on the other hand rather has a potential in the production and optimization process of naproxen than in the processes involving ibuprofen.

Determination of the kinetic parameters revealed that the activities of recombinant EstA and EstB are functions of substrate concentration as described by Michaelis-Menten kinetics, suggesting that the active site of neither of these enzymes is covered by a structural lid. This lid has been reported as a typical feature for lipases (Jaeger et al. 1994), and the determined kinetics therefore support the substrate-based characterization of EstA and EstB as esterases.

Industrial processes proceed often under high temperatures and the majority of known enzymes need to be stabilized under these conditions; therefore, there is a great interest in enzymes that are derived from extremophiles and stable without pretreatment (Huddleston et al. 1995; Bull et al. 1999; Morana et al. 2002; Mandrich et al. 2006). At 90°C EstA and EstB displayed a half-life ($t_{1/2}$) of 21 and 10 h, respectively. No significant reduction in activity was observed for EstA or EstB at 50°C. Manco and colleagues investigated the thermostability of esterase Est1 and Est2 from the Bacterium *A. acidocaldarius*. Est2 had a $t_{1/2}$ of 10 min at 90°C and 30% of the initial activity was recovered after Est1 had been incubated for 90 min at 75°C (Manco et al. 1994, 1998). Sobek and Gorisch reported that the residual activity of the *S. acidocaldarius* esterase declined to 92% after the purified enzyme had been incubated for 1 h at 90°C (Sobek and Gorisch 1988). These results provide strong evidence that EstA and EstB from *P. torridus* are valuable biocatalysts with unique properties for large-scale applications at high temperatures and during which a fluctuation of temperature and pH is inevitable.

Both recombinant esterases studied during this work were found to be active over a broad pH. Based on the intracellular pH of 4.6 it was assumed that many of the intracellular proteins of *Picrophilus* spp. would be maximally active under acidic conditions. Maximal activities of intracellular proteins from *P. torridus*, however, were measured around neutrality or at slightly acidic conditions, whereas the determined acidophilicity for extracellular proteins isolated from *Picrophilus* spp. was much more prominent (Serour and Antranikian 2002; Chen et al. 2006; Schepers et al. 2006). This is not surprising as proteins secreted by *Picrophilus* spp. have to withstand much higher concentrations of hydrogen ions. Considering the high activity of EstB under optimal conditions in vitro (2,639 U/mg), it is most likely that its activity is sufficient to catalyze the desired reaction at a physiological pH value of 4.6. In addition, it seems likely that the physiological substrates of EstA and EstB might be different from the substrates used for the characterization, and that *P. torridus* has a molecular machinery [e.g. heat shock proteins (HSPs)] to facilitate enzyme activity at lower pH values. The importance of HSPs for acidophilicity was demonstrated by recent studies devoted to the mechanisms responsible for the acidophilicity of *Oenococcus oeni* (Morel et al. 2001; Bourdineaud et al. 2003).

The potential capacity of EstA and EstB to hydrolyze fatty acid esters in organic solvents was investigated during this work and revealed that both esterases were active after pre-incubation with 50% (v/v) of various solvents and a significant increase in activity of EstA was found in the presence of dimethylformamide and toluol. Correspondingly, the thermophilic *A. nitroguajacolicus* esterase was activated by acetone, methanol, and diethylether (Schutte and Fetzner 2007). The ability of EstA and EstB to hydrolyze fatty acid esters in the presence of various organic solvents provides strong evidence that these esterases are of great interest for organic syntheses.

Acknowledgments This work was supported by grant 04-008 202131 from the German BMBF. We would like to thank Dr. Maryna Royter and Dr. Christian Elend for their support.

References

Altschul SF, Lipman DJ (1990) Protein database searches for multiple alignments. Proc Natl Acad Sci USA 87:5509–5513

Altschul SF, Madden TL, Schaffer AA, Zhang J, Zhang Z, Miller W, Lipman DJ (1997) Gapped BLAST and PSI-BLAST: a new generation of protein database search programs. Nucleic Acids Res 25:3389–3402

Arpigny JL, Jaeger KE (1999) Bacterial lipolytic enzymes: classification and properties. Biochem J 343(Pt 1):177–183

Bates PA, Kelley LA, MacCallum RM, Sternberg MJ (2001) Enhancement of protein modeling by human intervention in applying the automatic programs 3D-JIGSAW and 3D-PSSM. Proteins Suppl 5:39–46

Bell PJ, Sunna A, Gibbs MD, Curach NC, Nevalainen H, Bergquist PL (2002) Prospecting for novel lipase genes using PCR. Microbiology 148:2283–2291

Bendtsen JD, Nielsen H, von Heijne G, Brunak S (2004) Improved prediction of signal peptides: SignalP 3.0. J Mol Biol 340:783–795

Bernstein HJ (2000) Recent changes to RasMol, recombining the variants. Trends Biochem Sci 25:453–455

Berriman M, Rutherford K (2003) Viewing and annotating sequence data with Artemis. Brief Bioinform 4:124–132

Bornscheuer UT (2002) Microbial carboxyl esterases: classification, properties and application in biocatalysis. FEMS Microbiol Rev 26:73–81

Bourdineaud JP, Nehme B, Tesse S, Lonvaud-Funel A (2003) The *fts*H gene of the wine bacterium *Oenococcus oeni* is involved in protection against environmental stress. Appl Environ Microbiol 69:2512–2520

Bradford MM (1976) A rapid and sensitive method for the quantitation of microgram quantities of protein utilizing the principle of protein-dye binding. Anal Biochem 72:248–254

Britton HTS, Robinson RA (1931) Universal buffer solutions and the dissociation constant of veronal. J Chem Soc 458:1456–1462

Bull AT, Bunch AW, Robinson GK (1999) Biocatalysts for clean industrial products and processes. Curr Opin Microbiol 2:246–251

Carvalho PdO, Contesini FJ, Bizaco R, Calafatti SA, Macedo GA (2006) Optimization of enantioselective resolution of racemic ibuprofen by native lipase from *Aspergillus niger*. J Ind Microbiol Biotechnol 33:713–718

Chen YS, Lee GC, Shaw JF (2006) Gene cloning, expression, and biochemical characterization of a recombinant trehalose synthase from *Picrophilus torridus* in *Escherichia coli*. J Agric Food Chem 54:7098–7104

Ciaramella M, Napoli A, Rossi M (2005) Another extreme genome: how to live at pH 0. Trends Microbiol 13:49–51

De Simone G, Galdiero S, Manco G, Lang D, Rossi M, Pedone C (2000) A snapshot of a transition state analogue of a novel thermophilic esterase belonging to the subfamily of mammalian hormone-sensitive lipase. J Mol Biol 303:761–771

Demirjian DC, Moris-Varas F, Cassidy CS (2001) Enzymes from extremophiles. Curr Opin Chem Biol 5:144–151

Dharmsthiti S, Pratuangdejkul J, Theeragool GT, Luchai S (1998) Lipase activity and gene cloning of *Acinetobacter calcoaceticus* LP009. J Gen Appl Microbiol 44:139–145

Di Giulio M (2005) Structuring of the genetic code took place at acidic pH. J Theor Biol 237:219–226

Dutta S, Berman HM (2005) Large macromolecular complexes in the Protein Data Bank: a status report. Structure 13:381–388

Ejima K, Liu J, Oshima Y, Hirooka K, Shimanuki S, Yokota Y, Hemmi H, Nakayama T, Nishino T (2004) Molecular cloning and characterization of a thermostable carboxylesterase from an archaeon, *Sulfolobus shibatae* DSM5389: non-linear kinetic behavior of a hormone-sensitive lipase family enzyme. J Biosci Bioeng 98:445–451

Finn RD, Mistry J, Schuster-Bockler B, Griffiths-Jones S, Hollich V, Lassmann T, Moxon S, Marshall M, Khanna A, Durbin R et al (2006) Pfam: clans, web tools and services. Nucleic Acids Res 34:D247–D251

Fischer M, Thai QK, Grieb M, Pleiss J (2006) DWARF—a data warehouse system for analyzing protein families. BMC Bioinformatics 7:495

Futterer O, Angelov A, Liesegang H, Gottschalk G, Schleper C, Schepers B, Dock C, Antranikian G, Liebl W (2004) Genome sequence of *Picrophilus torridus* and its implications for life around pH 0. Proc Natl Acad Sci USA 101:9091–9096

Gasteiger E, Gattiker A, Hoogland C, Ivanyi I, Appel RD, Bairoch A (2003) ExPASy: The proteomics server for in-depth protein knowledge and analysis. Nucleic Acids Res 31:3784–3788

GOLD (2006) The Genomes On Line Database. Available at http://www.genomesonline.org. Accessed October 11 2006

Golyshina OV, Golyshin PN, Timmis KN, Ferrer M (2006) The 'pH optimum anomaly' of intracellular enzymes of *Ferroplasma acidiphilum* . Environ Microbiol 8:416–425

Hotelier T, Renault L, Cousin X, Negre V, Marchot P, Chatonnet A (2004) ESTHER, the database of the alpha/beta-hydrolase fold superfamily of proteins. Nucleic Acids Res 32:D145–D147

Hotta Y, Ezaki S, Atomi H, Imanaka T (2002) Extremely stable and versatile carboxylesterase from a hyperthermophilic archaeon. Appl Environ Microbiol 68:3925–3931

Huddleston S, Yallop CA, Charalambous BM (1995) The identification and partial characterisation of a novel inducible extracellular thermostable esterase from the archaeon *Sulfolobus shibatae*. Biochem Biophys Res Commun 216:495–500

Jaeger KE, Ransac S, Dijkstra BW, Colson C, van Heuvel M, Misset O (1994) Bacterial lipases. FEMS Microbiol Rev 15:29–63

Jaeger KE, Dijkstra BW, Reetz MT (1999) Bacterial biocatalysts: molecular biology, three-dimensional structures, and biotechnological applications of lipases. Annu Rev Microbiol 53:315–351

Kim S, Lee SB (2004) Thermostable esterase from a thermoacidophilic archaeon: purification and characterization for enzymatic resolution of a chiral compound. Biosci Biotechnol Biochem 68:2289–2298

Laemmli UK (1970) Cleavage of structural proteins during the assembly of the head of bacteriophage T4. Nature 227:680–685

Manco G, Di Gennaro S, De Rosa M, Rossi M (1994) Purification and characterization of a thermostable carboxylesterase from the thermoacidophilic eubacterium *Bacillus acidocaldarius*. Eur J Biochem 221:965–972

Manco G, Adinolfi E, Pisani FM, Ottolina G, Carrea G, Rossi M (1998) Overexpression and properties of a new thermophilic and thermostable esterase from *Bacillus acidocaldarius* with sequence similarity to hormone-sensitive lipase subfamily. Biochem J 332(Pt 1):203–212

Manco G, Camardella L, Febbraio F, Adamo G, Carratore V, Rossi M (2000) Homology modeling and identification of serine 160 as nucleophile of the active site in a thermostable carboxylesterase from the archaeon *Archaeoglobus fulgidus*. Protein Eng 13:197–200

Mandrich L, Pezzullo M, Rossi M, Manco G (2006) SSoNΔ and SSoNΔlong: two thermostable esterases from the same ORF in the archaeon *Sulfolobus solfataricus*? Archaea 2:1–7

Margolin AL (1993) Enzymes in the synthesis of chiral drugs. Enzyme Microb Technol 15:266–280

Morana A, Di Prizito N, Aurilia V, Rossi M, Cannio R (2002) A carboxylesterase from the hyperthermophilic archaeon *Sulfolobus solfataricus*: cloning of the gene, characterization of the protein. Gene 283:107–115

Morel F, Delmas F, Jobin MP, Divies C, Guzzo J (2001) Improved acid tolerance of a recombinant strain of *Escherichia coli* expressing genes from the acidophilic bacterium *Oenococcus oeni*. Lett Appl Microbiol 33:126–130

Park YJ, Choi SY, Lee HB (2006) A carboxylesterase from the thermoacidophilic archaeon *Sulfolobus solfataricus* P1; purification, characterization, and expression. Biochim Biophys Acta 1760:820–828

Rhee JK, Ahn DG, Kim YG, Oh JW (2005) New thermophilic and thermostable esterase with sequence similarity to the hormone-sensitive lipase family, cloned from a metagenomic library. Appl Environ Microbiol 71:817–825

Sambrook J, Fritsch EF, Maniatis T (1989) Molecular cloning: a laboratory manual, 2nd edn. Cold Spring Harbor Laboratory Press, Cold Spring Harbor

Sanger F, Nicklen S, Coulson AR (1977) DNA sequencing with chain-terminating inhibitors. Proc Natl Acad Sci USA 74:5463–5467

Sayle RA, Milner-White EJ (1995) RASMOL: biomolecular graphics for all. Trends Biochem Sci 20:374

Schepers B, Thiemann V, Antranikian G (2006) Characterization of a novel glucoamylase from the thermoacidophilic Archaeon *Picrophilus torridus* heterologously expressed in *E. coli*. Eng Life Sci 6:311–317

Schmidt-Dannert C, Sztajer H, Stocklein W, Menge U, Schmid RD (1994) Screening, purification and properties of a thermophilic lipase from *Bacillus thermocatenulatus*. Biochim Biophys Acta 1214:43–53

Schomburg I, Chang A, Ebeling C, Gremse M, Heldt C, Huhn G, Schomburg D (2004) BRENDA, the enzyme database: updates and major new developments. Nucleic Acids Res 32:D431–D433

Schutte M, Fetzner S (2007) EstA from *Arthrobacter nitroguajacolicus* Ru61a, a thermo- and solvent-tolerant carboxylesterase related to Class C beta-lactamases. *Curr Microbiol*

Serour E, Antranikian G (2002) Novel thermoactive glucoamylases from the thermoacidophilic Archaea *Thermoplasma acidophilum*, *Picrophilus torridus* and *Picrophilus oshimae* . Antonie Van Leeuwenhoek 81:73–83

Sobek H, Gorisch H (1988) Purification and characterization of a heat-stable esterase from the thermoacidophilic archaebacterium *Sulfolobus acidocaldarius*. Biochem J 250:453–458

Suzuki Y, Miyamoto K, Ohta H (2004) A novel thermostable esterase from the thermoacidophilic archaeon *Sulfolobus tokodaii* strain 7. FEMS Microbiol Lett 236:97–102

Thompson JD, Higgins DG, Gibson TJ (1994) CLUSTAL W: improving the sensitivity of progressive multiple sequence alignment through sequence weighting, position-specific gap penalties and weight matrix choice. Nucleic Acids Res 22:4673–4680

Thompson JD, Gibson TJ, Plewniak F, Jeanmougin F, Higgins DG (1997) The CLUSTAL_X windows interface: flexible strategies for multiple sequence alignment aided by quality analysis tools. Nucleic Acids Res 25:4876–4882

Vossenberg vd, Driessen AJ, Zillig W, Konings WN (1998) Bioenergetics and cytoplasmic membrane stability of the extremely acidophilic, thermophilic archaeon *Picrophilus oshimae*. Extremophiles 2:67–74

Winkler UK, Stuckmann M (1979) Glycogen, hyaluronate, and some other polysaccharides greatly enhance the formation of exolipase by *Serratia marcescens*. J Bacteriol 138:663–670